Astron. Astrophys. 294, 232–240 (1995)

ASTRONOMY AND ASTROPHYSICS

Acoustic wave propagation in the solar atmosphere

I. Linear response to adiabatic wave excitation

G. Sutmann and P. Ulmschneider

Institut für Theoretische Astrophysik der Universität Heidelberg, Im Neuenheimer Feld 561, D-69120 Heidelberg, Germany

Received 16 March 1994 / Accepted 27 July 1994

Abstract. We study the response of various solar atmosphere models to excitation by adiabatic small amplitude acoustic waves. Both monochromatic waves and acoustic spectra are considered. We find that upon excitation, strong resonance oscillations of a single frequency develop which are superposed over the excitation signal. These resonances decay exponentially with time; the decay rate varies strongly with the temperature gradient of the model. In realistic and positive gradient atmospheres the decay rate is much faster than in isothermal models, while in negative gradient models it is even slower. Independent of whether the atmosphere is excited by a pulse or by continuous wave action a similar decay behaviour is found. The response to a stochastic wave spectrum is a series of uncorrelated transient events, each with the associated exponential decay of the resonance.

Key words: hydrodynamics – waves – Sun: chromosphere – Sun: oscillations

1. Introduction

Although the dominant oscillatory signal in the solar photosphere is the 5-min oscillation discovered by Leightonet al. (1962), the pronounced signal in the solar chromosphere observed in the Ca II H and K, Hα and the Ca II infrared triplet lines is one near 3 min (ν = 5.5 mHz). For detailed reviews of the 3 min oscillation see Deubner (1991), Fleck & Schmitz (1991) as well as Rutten & Uitenbroek (1991). The numerous analytical and numerical investigations prior to 1980 concerning the dynamic response of the chromosphere to various excitations, in which the resonance character of the atmosphere was noticed, have been discussed by Fleck & Schmitz (1991).

As the interpretation of 5 min oscillations as trapped subphotospheric eigenmodes was very successful and even opened up an entirely new branch of astrophysics, the field of asteroseismology, the idea appeared very attractive that the chromospheric 3 min oscillation might be likewise explained by a chromospheric cavity, acting between the temperature minimum and the foot of the chromosphere-corona transition layer (Leibacher & Stein 1981). Yet it now appears that this view is incorrect. Fleck & Schmitz (1991) were the first to show that the 3-min oscillation, instead of being a cavity mode, might be explained much more simply as the basic cut-off frequency resonance of the chromosphere.

The difference of a resonance and a cavity mode is that a cavity mode is dominated by its finite width, into which only waves of certain frequencies fit, while a resonance does not depend on such a width. On the contrary, the atmospheric resonance is the response of the atmosphere to a local perturbation of gas elements out of their rest position in hydrostatic equilibrium. Atmospheric resonances usually occur in the wake of a strong disturbance which propagates through the atmosphere. Resonant oscillations are independent of any cavity width because they occur already much before the head of a strong disturbance has reached some hypothetical cavity boundary (see Figs. 4 and 6, below, where resonances occur already much before the transit time of the atmosphere, which is roughly 300 s).

It could be shown that the linearized hydrodynamic equations under adiabatic conditions in a gravitationally stratified, isothermal atmosphere lead to a Klein-Gordon equation (Morse & Feshbach 1953, p. 139) which is a special form of the telegraph equation (Courant & Hilbert 1962, p. 192). Numerically evaluating analytic solutions for sinusoidal oscillations which started at time $t = 0$ in an initially undisturbed isothermal atmosphere, Fleck & Schmitz (1991) were able to show that the atmosphere gave a 3-min type resonant response in absence of any cavity. This response was also confirmed with time-dependent numerical calculations in finite slabs of an isothermal atmosphere. These authors moreover showed that the resonance character was essentially the same when a realistic atmosphere model (Vernazza et al. 1981, model C) was taken. This great success in our understanding of the 3-min oscillation was further supported and elucidated by Kalkofen et al. (1994) who were able to give a simple analytical solution which showed in great detail the spatial and temporal behaviour of the velocity amplitude of acoustic waves excited in an isothermal gravitational atmosphere.

Fleck & Schmitz (1993) as well as Kalkofen et al. (1994) also investigated the nonlinear response of various atmosphere

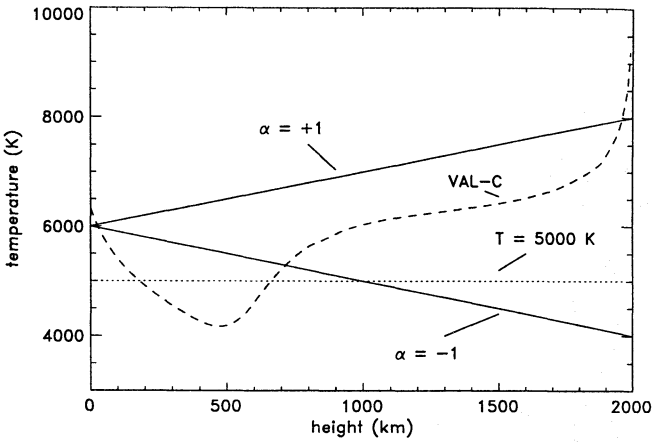

Fig. 1. Atmospheric models considered in this paper

models to adiabatic waves of large amplitude. Here the formation of shocks and shock overtaking occur. We will discuss and extend these results in a second paper of this series (Sutmann & Ulmschneider 1994).

In this present first paper we want to extend the linear wave studies by investigating the role which the atmospheric temperature gradient plays in the decay characteristics of the atmospheric resonance. We find that the chromospheric temperature gradient profoundly influences the resonance properties of the atmosphere. In Sect. 2 we discuss the time- dependent numerical methods which we use as well as the analytic results of Kalkofen et al. (1994). Section 3 presents our results while Sect. 4 gives a discussion. Section 5 brings our conclusions.

2. Method

2.1. The atmosphere models

For the investigation of atmospheric oscillations of the Sun suitable initial atmosphere models are necessary. Of these the isothermal models are of great interest, because they allow analytical studies. As we wanted to reproduce these analytic results numerically we selected an isothermal model with temperature T_o = 5000 K and height z = 2000 km which corresponds to about 17 scale heights. To study how the atmospheric model influences the response to oscillatory perturbations we also used polytropic atmospheres which are characterized by a constant temperature gradient $dT/dz = \alpha$ (Lamb 1908). We use atmosphere models with $\alpha = -1$, +1 K/km and also a height of z = 2000 km. Finally we employ the semiempirical atmosphere model C of Vernazza et al. (1981). All atmosphere models have solar gravity $g = 2.736 \cdot 10^4$ cm s^{-2} and are shown in Fig. 1.

2.2. The hydrodynamic computations

The computation of acoustic waves has been discussed in previous work (Ulmschneider et al. 1977; Ulmschneider et al. 1987; Rammacher & Ulmschneider 1992) and therefore does not need to be described again. For our present adiabatic work the radiation treatment is skipped. The time–dependent hydrodynamic equations are solved for an atmospheric slab using the method of characteristics. At the top of the atmosphere a transmitting boundary is used while at the bottom, disturbances are introduced by means of a piston.

In our present investigation we excite with waves of extremely small amplitude to make sure that we avoid shocks and to be able to compare our results with linear analytic solutions. As shock formation is particularly easy in extended atmospheres and for high frequency waves, we restrict our investigations to low frequency waves and to cases where the width of the atmospheric slab is sufficiently small.

2.3. The bottom boundary condition

At the bottom boundary, velocity fluctuations are prescribed by using a piston. To study the response of the atmosphere to different types of piston motions, we have chosen four types of velocity functions:

a) long period continuous sinusoidal oscillations with a frequency below the cut-off frequency (cf. Eq. (10))

$$u_0(t) = Mc\sin(\omega t) \quad , \tag{1}$$

where $\omega = 2\pi\nu$ is the circular frequency, t the time, M the Mach number and c the sound speed,

b) pulse excitation, which can be described as a sinusoidal wave with period P_0, where the piston is stopped after one period. This kind of movement can be seen as superposition of two sinusoidal waves with a phase lag of one period

$$u_0(t) = Mc\ \left(\mathscr{H}(t) - \mathscr{H}(t - P_0)\right)\sin(\omega t) \quad , \tag{2}$$

where $\mathscr{H}(t)$ is the Heaviside step function which is defined by

$$\mathscr{H}(t) = \begin{cases} 0 & t < 0 \\ 1 & t \geq 0 \end{cases} \quad , \tag{3}$$

and $\omega = 2\pi/P_0$,

c) wave spectra, which are constructed by superposing sinusoidal waves with frequency ω_n. The amplitudes of the partial waves are distributed in a Gaussian manner

$$u_0(t) = c\sum_{n=0}^{N} M_n \sin(\omega_n t + \varphi_n) \quad , \tag{4}$$

where φ_n is a constant but arbitrary phase, N = 100 and

$$M_n = M\exp\left\{-\frac{(\omega_n - \omega_C)^2}{2\omega_\sigma^2}\right\} \quad , \tag{5}$$

is the Gaussian distributed Mach number of the partial waves. $\omega_C = \omega_{N/2} = 2\pi\nu_C$ is the central frequency and ω_σ is the width of the function. The constant frequency interval was chosen as $\Delta\omega = \omega_{i+1} - \omega_i = 2\pi\ 5 \cdot 10^{-5}\ Hz$.

d) stochastically generated wavetrains, which result from changing the frequency stochastically after each period. The moving piston can be described by superposing sinusoidal waves

$$u_0(t) =$$

$$Mc \sum_{n=1}^{N} \left[\left\{ \mathscr{H}(t - \sum_{i=0}^{n-1} P_i) - \mathscr{H}(t - \sum_{i=0}^{n} P_i) \right\} \sin(\omega_n t) \right] \quad (6)$$

with

$$P_0 = 0 \quad , \quad P_n = \frac{2\pi}{\omega_n} \quad , \quad \omega_n = Z_n \, \omega_M \quad , \quad (7)$$

where $Z_n \in [0, 1]$ is a random number, ω_M the maximum frequency and N is found from the condition that $\sum P_i > t$.

2.4. Fourier analysis

For the Fourier analysis of velocity fluctuations at different heights of the atmosphere it is necessary to take a fixed Eulerian grid in space and an equidistant grid in time. Because our hydrodynamic code works in the Lagrange frame and as the time step is chosen according to the Courant condition, we interpolated the velocity both in space and time. The interpolation is done by the method of weighted parabolas, described by Ulmschneider et al. (1977). The equidistant time interval is chosen as 1 s, the height interval as 100 km. The time interval for the Fourier analysis is always 2000 s which gives a frequency resolution of $\Delta\nu = 0.5$ mHz.

2.5. Asymptotic solution for the isothermal case

Following Lamb (1908, 1932), Kalkofen et al. (1994) showed that the response of an isothermal atmosphere to a continuous excitation by the velocity oscillation

$$u_0(t) = Mc \, \mathrm{e}^{-i\omega t} \quad , \quad (8)$$

which starts at time $t = 0$ is asymptotically given by

$$u(z,t) = Mc \left\{ \mathrm{e}^{-i(\omega t - \sqrt{\omega^2 - \omega_A^2}\, z/c)} - \sqrt{\frac{2\omega_A}{\pi c^2}} \frac{z}{t^{3/2}(\omega_A^2 - \omega^2)} \right.$$

$$\left. \cdot \left[\omega_A \sin\left(\omega_A t - \frac{3}{4}\pi\right) + i\omega \cos\left(\omega_A t - \frac{3}{4}\pi\right) \right] \right\} \mathrm{e}^{z/(2H)} \quad , (9)$$

for $t >> z/c$. Here z is height, ω the circular frequency, H the scale height, $M << 1$ the Mach number,

$$\omega_A = \frac{\gamma g}{2c} = \frac{c}{2H} \quad , \quad (10)$$

the acoustic cut-off frequency and

$$c = \sqrt{\gamma R T_o / \mu} \quad , \quad (11)$$

the sound speed with $R = 8.31 \cdot 10^7$ erg grad^{-1}mol^{-1} the universal gas constant, $\mu = 1.3$ g/mol the mean molecular weight and $\gamma = 5/3$ the ratio of specific heats for neutral gases. Note that different to Kalkofen et al. we use a "-"-sign in Eq. (8) which leads to the correct expression in Eq. (9) for evanescent waves which are exponentially damped compared to propagating waves. As discussed by Kalkofen et al. (1994), Eq. (9) consists of two contributions, the exciting wave with frequency ω and a resonance oscillation around the cut-off frequency ω_A. This resonance contribution vanishes for large times t due to the $t^{-3/2}$ term. Depending on whether ω is greater or less than ω_A, the exciting wave contribution is propagating or evanescent, respectively. The contributions have a z-dependence and in addition, due to energy conservation, the wave amplitudes of both contributions grow with height like $e^{z/(2H)}$. This means that for the exciting contribution there will always be a net growth with height, even in the evanescent case, except for $\omega \to 0$, where the amplitude stays constant with height.

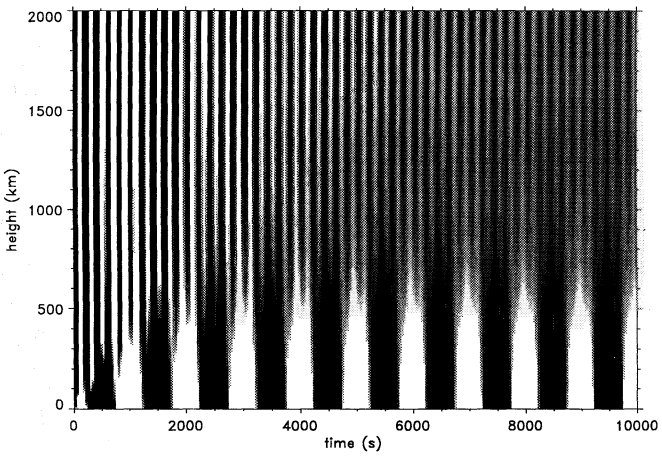

Fig. 2. Height-time plot for oscillations in an isothermal atmosphere with cut-off frequency $\nu_A = 5.0$ mHz for an excitation frequency of $\nu = 1$ mHz. For the presentation the global $\exp(z/(2H))$ term has been removed

As we later want to investigate the different response of non-isothermal atmospheres, we discuss the complicated behaviour of Eq. (9) in more detail by using a graphical representation. Figures 2, 3 show the velocity given by Eq. (9) for excitation frequencies $\nu = \omega/(2\pi) = 1$ and 10 mHz. Actually Figs. 2, 3 display the velocity with the global $e^{z/(2H)}$ term removed. From Eqs. (10), (11) with $T_o = 5000$ K the cut-off frequency is $\nu_A = \omega_A/(2\pi) = 5.0$ mHz. The figures display velocities by increasing density of grayness such that negative velocities are shown white and positive velocities black.

Figure 2 shows the case of an excitation by oscillations of frequency $\nu = 1$ mHz. As this frequency is below the cut-off frequency, the wave is evanescent and is damped as function of height. Figure 2 shows the incident wave with frequency ν at height $z = 0$ km. For a fixed time, but increasing height z, it is seen that the exponentially damped excitation component gets more and more replaced by the resonance contribution which grows with height. On the other hand, for a fixed height (say $z = 500$ km) the resonance oscillation dies out for increasing times due to the $t^{-3/2}$ dependence and only the exciting wave survives, weakened due to its exponential damping with height. As both the resonance oscillation and the incident evanescent wave have infinite phase speed the stripes in Fig. 2 are vertical.

The case with $\nu = 10$ mHz $> \nu_A$ is that of an excitation by a propagating wave. The resonance oscillation with ν_A shown at the left hand side in Fig. 3, is kicked on by the initial disturbance

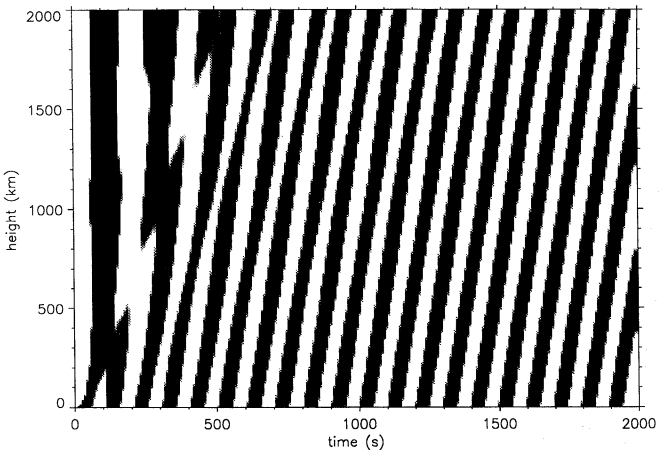

Fig. 3. Same as Fig. 2 however for an excitation frequency of ν = 10 mHz. For the presentation the global $\exp(z/(2H))$ term has been removed

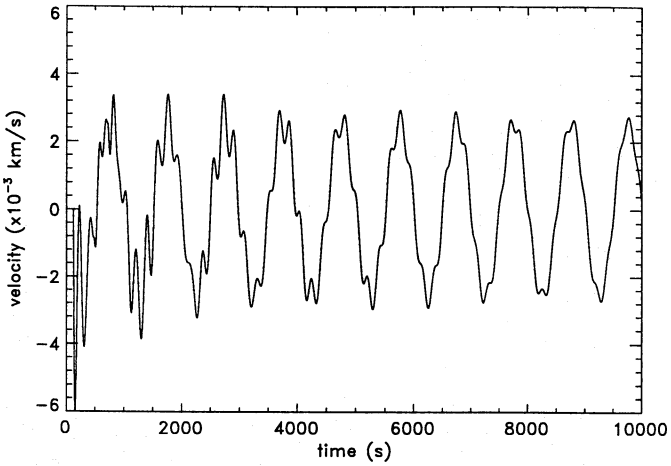

Fig. 4. Velocity oscillation as a function of time in an isothermal atmosphere with T_o = 5000 K (resonance frequency ν_A = 5.0 mHz) continuously excited by a wave with frequency ν = 1 mHz. The oscillations are shown at an altitude of z = 800 km

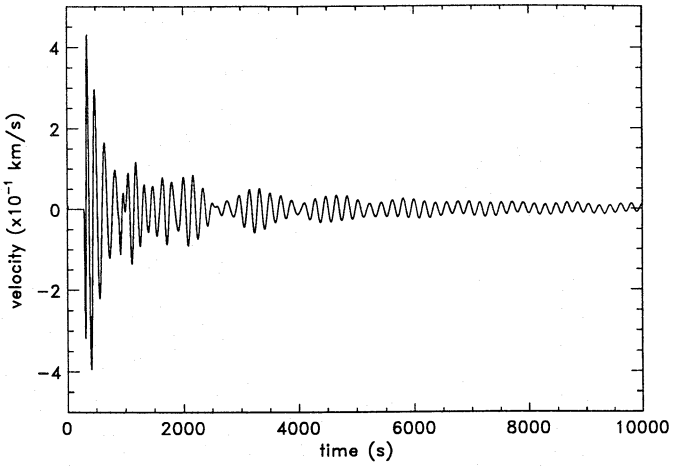

Fig. 5. Same as Fig. 4, but at an altitude of 2000 km

which moved into the undisturbed atmosphere. Here, as in Fig. 2, we have assumed that the head of the wave has already gone through the entire 2000 km height range, which is the condition for the validity of Eq. (9). At a given height the resonance dies out due to the $t^{-3/2}$-dependence and only the incident oscillation survives. As the resonance oscillation is increasingly important at greater z, its replacement by the incident excitation occurs at progressively later times. Thus the resonance oscillation with its infinite phase speed is confined to the upper left hand side of Fig. 3, while the propagating wave shows inclined stripes in agreement with its finite phase speed.

3. Results

In this section we discuss our adiabatic numerical studies which were performed using the time-dependent hydrodynamic code described above. As waves with realistic amplitudes, introduced at the bottom of the atmosphere, will grow to large amplitudes and form shocks, we keep the Mach number of the velocity excitation at the piston to very small values of between $M = 2.4 \cdot 10^{-4}$ and $4 \cdot 10^{-4}$. This is to ensure that in our atmospheric slab the oscillations remain in the linear regime even for short period waves, which generate shocks most easily.

3.1. The isothermal atmosphere

Our wave simulations in isothermal atmospheres of various temperature turned out to give rather similar results. For this reason we discuss only results for models with T_o = 5000 K. Figure 4 shows the time-development of oscillations in an isothermal atmosphere, continuously excited with a frequency ν = 1 mHz. The oscillations are shown at an altitude of z = 800 km (7 scale heights). It is seen that initially large resonance oscillations with ν_A = 5.0 mHz are superposed over the incident wave. As time progresses these resonance oscillations die out and the incident wave survives.

This behaviour is even more drastically seen in Fig. 5 which shows the same wave as in Fig. 4 but at an altitude of z = 2000 km (17 scale heights). In principle the waves in Fig. 5 show the same behaviour as in Fig. 4, or as that predicted by the asymptotic Eq. (9): the initially large amplitude of the resonance oscillation dies out with increasing time. Moreover, the amplitude of the resonance oscillation in Fig. 5 is much larger than that in Fig. 4, which is explained from the z-dependence in Eq. (9). It will take considerable additional time until the resonance oscillation has completely died out. Also notice in Figs. 4 and 5 the time lag between the start of the oscillations (with negative velocities) and the start of the computation at time t = 0 s. This time lag is due the transit time of the head of the wave through the undisturbed atmosphere.

Excitation of the isothermal atmosphere by a pulse is shown in Figs. 6 and 7. It is seen that the propagating pulse, which travels into the undisturbed atmosphere, generates a wake of resonance oscillations. The ideally infinite phase speed of the

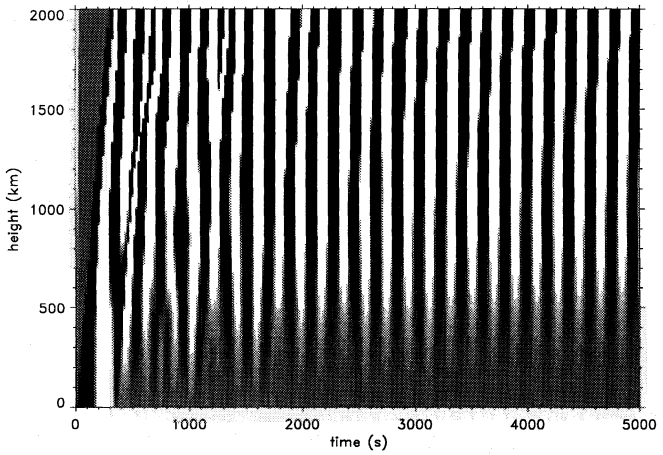

Fig. 6. Height-time plot for oscillations in an isothermal atmosphere with cut-off frequency ν_A = 5.0 mHz for an excitation by a pulse of 300 s duration

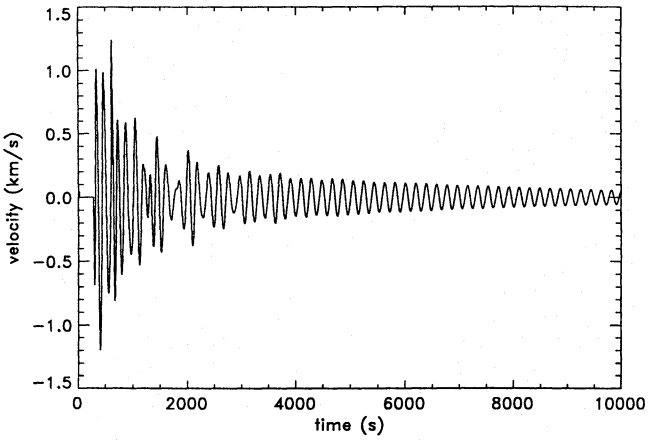

Fig. 7. Velocity oscillation as a function of time in an isothermal atmosphere with T_o = 5000 K excited by a pulse. The oscillations are shown at z = 2000 km height

resonance oscillations, shown as vertical stripes in Fig. 6, is seen to be perturbed by propagating disturbances which rapidly die out with time. Figure 7 shows the exponential time development of the velocity at height z = 2000 km.

In addition, Figs. 6 and 7 explain that the power spectrum of the oscillations has a characteristic time behaviour. We find that while the power in the time interval from 500 to 2500 s has peaks at frequencies 6 to 7 mHz, the power in the time interval from 7000 to 9000 s has only one peak at 5 mHz. This is understood from the propagating character of the pulse disturbance close to the start of the calculation. As seen in Fig. 6 the vertical stripes at the top left part of the diagram are inclined (finite phase speed) and squeezed together in the right hand direction, thus generating higher frequencies, while on the right part of this figure they are mainly vertical, corresponding to the basic resonance (5 mHz) of the isothermal atmosphere.

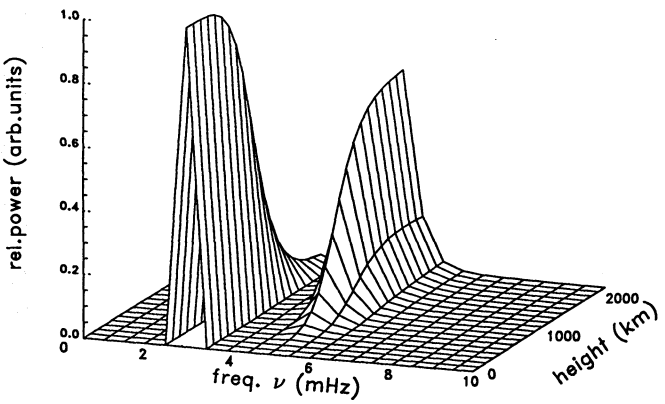

Fig. 8. Normalized power spectrum as a function of height for a polytropic atmosphere with negative temperature gradient, for times greater than 7000 s

3.2. Polytropic atmospheres with negative temperature gradient

We now discuss the polytropic atmospheres. As we find that polytropic atmospheres with negative and positive temperature gradients behave very differently, let us first discuss those with negative temperature gradients. For polytropic atmospheres there is no longer a unique cut-off frequency. At the bottom, where our model has a temperature of T = 6000 K, we have a cut-off frequency ν_A = 4.5 mHz, while at z = 2000 km height at a temperature of T = 4000 K, we have ν_A = 5.6 mHz. Let this atmosphere be continuously excited with a frequency of ν = 3.0 mHz. The power spectrum as a function of height for times greater than t = 6000 s is shown in Fig. 8. It is seen that the relative power of the exciting wave decreases, while that of the resonance oscillation increases with height. The important fact is, that despite different cut-off frequencies as functions of height, a common resonance frequency develops with a peak at ν = 5.0 mHz, which is typical for T = 5000 K, that is, the average atmospheric temperature.

In Fig. 8 the power has been normalized to one at every height to allow a comparison of the two (resonance and incident wave) contributions as a function of height. For later times the resonance contribution very slowly decreases and the contribution of the incident wave increases. Finally after a very long time only the exciting wave survives showing the left hand ridge with amplitude unity over the entire height and no right hand ridge in Fig. 8.

The excitation by a pulse in an atmosphere with negative temperature gradient is shown in Fig. 9. It is seen that the velocity behaves similarly as in the case of the isothermal atmosphere (Fig. 7). But the decay rate of the oscillation for long times is much reduced compared to the isothermal case. This seems to be a general property of negative gradient atmospheres as it is also found in the case of continuous excitation. Likewise, as in the case of a continuous excitation, a resonance at 5 mHz develops.

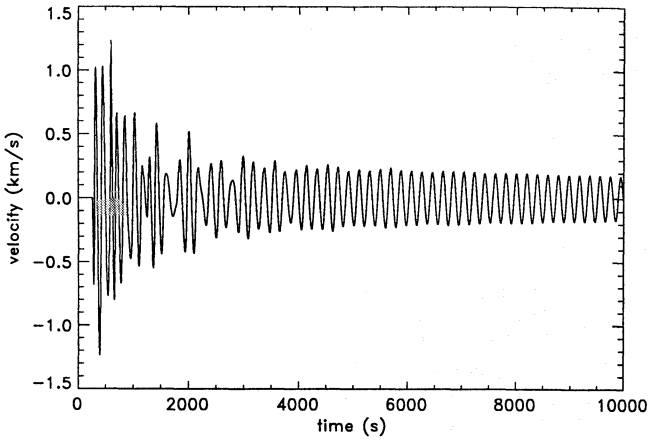

Fig. 9. Velocity oscillation as a function of time at height $z = 2000$ km in an atmosphere with negative temperature gradient, excited by a pulse

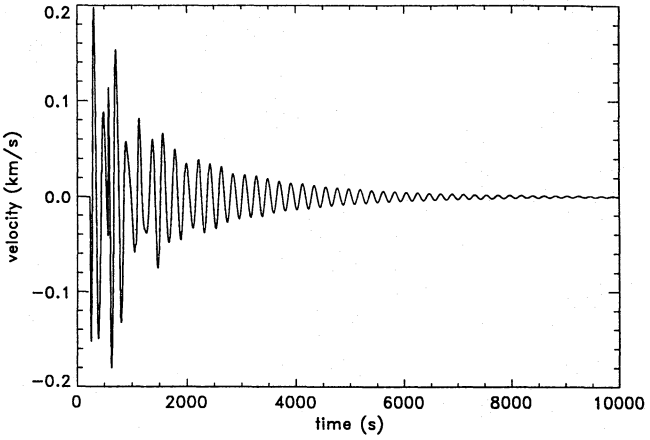

Fig. 11. Velocity oscillation as a function of time at height $z = 2000$ km in an atmosphere with positive temperature gradient, excited by a pulse

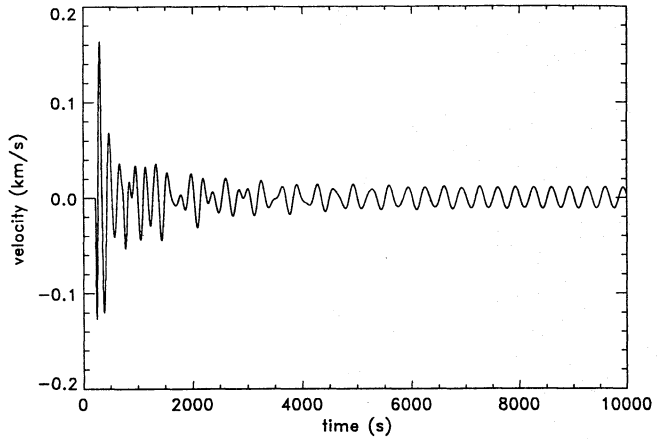

Fig. 10. Velocity oscillation as a function of time at height $z = 2000$ km in an atmosphere with positive temperature gradient, continuously excited by a wave of frequency $\nu = 3.0$ mHz

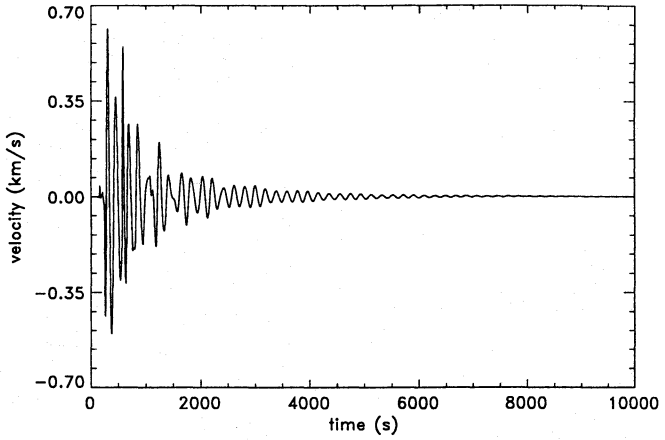

Fig. 12. Velocity oscillation as a function of time at height $z = 1900$ km in model C of Vernazza et al. (1981), excited by a pulse

3.3. Polytropic atmospheres with positive temperature gradient

We now discuss the polytropic atmosphere with a positive temperature gradient. Here at height $z = 2000$ km with temperature 8000 K one has a cut-off frequency of $\nu_A = 3.9$ mHz, while at $z = 0$ km one has $\nu_A = 4.5$ mHz. Figure 10 at height $z = 2000\ km$ shows the velocity oscillations as a function of time for a continuous excitation with a frequency of $\nu = 3.0$ mHz. Contrary to the isothermal or negative gradient cases, it is seen here that the resonance disturbance dies out very rapidly. At $z = 2000$ km after about $\Delta t \approx 6000$ s, essentially only the exciting wave remains. For lower heights $z = 400, 800, 1200, 1600$ km, these times are $\Delta t = 4000, 4500, 5000, 5500$ s, respectively.

This drastic decay behaviour is even more clearly seen in the pulse excitation. Figure 11 shows the essentially exponential decay of the resonance disturbance. A comparison of Fig. 11 with Figs. 7 and 9 shows that the temperature gradient greatly influences the decay characteristic of the atmospheric resonances. While isothermal atmospheres have a slow decay rate this rate is even slower for negative temperature gradient atmospheres but very much faster for atmospheres with positive temperature gradients. Also note that the initial oscillation amplitude of the resonance in the positive gradient atmosphere is greatly reduced compared to that in the other two cases.

Another important result of both wave calculations in atmospheres with a positive temperature gradient is that, despite a dependence of ν_A with height, again a resonance oscillation with a common frequency $\nu = 4.5$ mHz develops, which, different from the atmosphere with a negative temperature gradient, is equal to that of the lowest, most massive layer.

3.4. The Vernazza et al. model

We finally investigate the response properties of a realistic solar model. Figure 12 displays the time-development of the velocity oscillations at $z = 1900$ km height due to an excitation with a pulse. Comparison with Figs. 7, 9 and 11 shows that realistic atmospheres have the very rapid resonance decay characteristics common to atmospheres with a positive temperature gradient which is very unlike to that of the isothermal or neg-

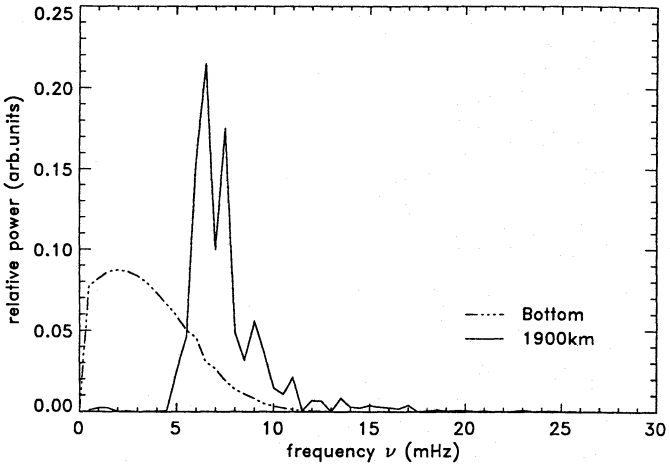

Fig. 13. Power spectrum for excitation by a Gaussian acoustic spectrum centered in the nonpropagating region for model C of Vernazza et al. (1981). The input power at the bottom of the atmosphere is shown dashed while that at z = 1900 km height is shown drawn

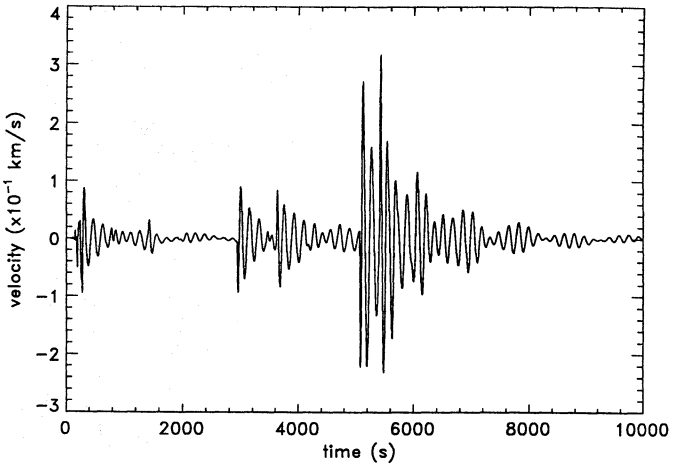

Fig. 14. Velocity oscillation as a function of time at height z = 1900 km in model C of Vernazza et al. (1981), excited by a stochastic wave spectrum where all frequencies are below the cut-off frequency

ative temperature gradient atmospheres. For a pulse excitation we found that after times greater than 2500 s, despite a height-dependent ν_A, a common resonance oscillation with frequency ν = 5 mHz develops. The power spectrum for continuous excitation, however, showed a marked time dependence. For times between 500 and 2500 s a double peak at 5 and 6 mHz developed at great heights. In subsequent times the 5 mHz peak became more important while, similarly to the cases discussed for other atmosphere models, both peaks rapidly decayed compared to that of the incident frequency. Consistently with the positive temperature gradient case, both wave calculations show much reduced initial amplitudes of the resonances compared with the isothermal and negative temperature gradient cases. This indicates that for atmospheric oscillation studies, isothermal and negative temperature gradient atmospheres should be avoided.

3.5. Evanescent and propagating behaviour

Very instructive for the understanding of the energy transport in stellar chromospheres is to compute a Gaussian spectrum which has contributions both above and below the cut-off frequency. To avoid shock formation of the high frequency components and to assure linearity, we have chosen the central frequency ν_C = 2 mHz in the nonpropagating region $\omega < \omega_A$ and select $\omega_\sigma = \omega_A/10$ to give only a slight overlap with the propagating region. Figure 13 shows that the power at z = 1900 km height in model C of Vernazza et al. (1981) in the nonpropagating region $\nu < 5$ mHz is essentially zero, while a large amount of power is present in the propagating region $\nu > 5$ mHz. This is due to the fact that the evanescent parts of the spectrum are exponentially damped, while the propagating parts are exponentially amplified. Figure 13 thus shows that the atmosphere can be considered as a high pass filter. Note that because we wanted to study the linear behaviour, we have largely avoided the propagating frequency range in our present paper. It will be addressed in Paper II of this series.

3.6. Stochastic excitation

Excitation by a stochastic wave spectrum is probably more realistic because it simulates the character of an uncorrelated series of transient events. Figure 14 shows the velocity at z = 1900 km height in model C of Vernazza et al. (1981) for an excitation given by Eq. (6) where $\omega_M = 2\pi \cdot 3.3$ mHz is below the cut-off-frequency. We find, see Fig. 14, that each change in frequency is accompanied by a new resonance oscillation together with its associated decaying wave train at the cut-off frequency.

4. Discussion

A first point of our discussion is the question of the agreement of our numerical computations with the analytical results. There are two main differences between the two approaches. The first is that the analytic case considers an atmosphere with infinite extent while the numerical case uses an atmosphere with finite extent and a transmitting boundary condition. The second difference is that the analytic result rests on expansions where only the first terms were retained and, moreover, which is valid only for large times. Fleck & Schmitz (1991) were able to numerically evaluate analytical solutions both for a semi-infinite and a finite slab. They found that the general behaviour of the solution was not affected by the finite slab width, despite the fact that their case had a rigid upper boundary condition which, due to the many reflections, contributed to a very noisy appearance of the wave field (see their Fig. 2). Our time-dependent computations did not show any noticeable difference to the behaviour shown in their Fig. 1 and for times $t > 2000$ s to our Fig. 2. This we attribute to the fact that our transmitting boundary condition works very well for linear waves. The second difference is more difficult to assess.

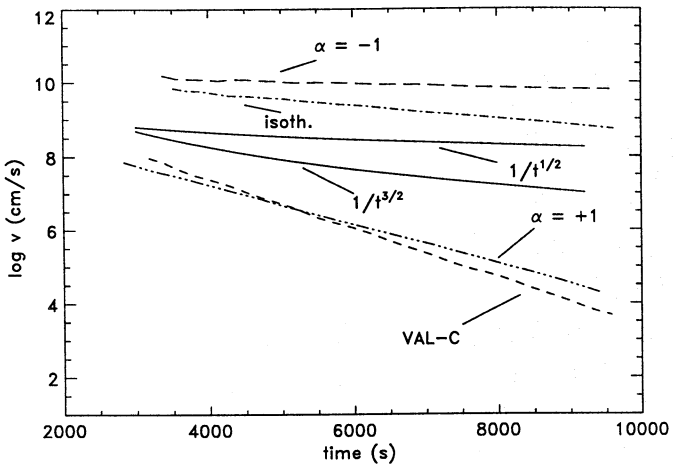

Fig. 15. Decay of the averaged velocity amplitude of the wave crests with time in the case of the pulse excitation. Shown are the isothermal atmosphere with T_0 = 5000 K, the polytropic atmospheres with positive and negative temperature gradients α and model C of Vernazza et al. (1981). Also shown is the decay behaviour concerning a power-law as well $u \propto t^{-1/2}$ as $u \propto t^{-3/2}$ (The initial amplitudes of the power-laws are arbitrarily chosen)

From roughly 30 wave crests we are able to measure the damping rate of the velocity in our numerical calculations. The obtained decay behaviour of the velocity amplitudes is shown in Fig. 15. It is seen that in the timespan of our computations these decay curves are best represented by an exponential damping law $u(t) \sim e^{-\delta t}$, where for $\delta = 1.8 \cdot 10^{-4}, 5.8 \cdot 10^{-5}, 5.4 \cdot 10^{-4}, 6.7 \cdot 10^{-4}$ s^{-1} for the isothermal atmosphere, the negative and positive temperature gradient atmosphere and for model C of Vernazza et al. (1981), respectively. Moreover, for an atmosphere with $dT/dz = 0.5$ K/km we find $\delta = 4.2 \cdot 10^{-4}$ s^{-1}.

This agrees quite well with the visual appearance of the decay of the resonances in all our Figs. (4, 5, 7, 9, 10, 11, 12, 14) and suggests that the $t^{-3/2}$ law found by Kalkofen et al. (1994) may be only an approximation to a universal exponential decay law for the resonances excited in the atmosphere. This view is also supported by a comparison of the $t^{-3/2}$ law with our exponential results for the isothermal atmosphere as shown in Fig. 15. It is seen that both laws behave rather similarly. We thus suspect that the $t^{-3/2}$ law is an artifact of the approximations made in the analytical derivation and that in reality the resonances decay exponentially both over short and long time scales. This is also what one would naively expect. Unfortunately we are not able at the present time to show this with a more sophisticated analytical derivation.

A second point to be discussed is the difference in the decay behaviour found between a pulse excitation and a continuous wave excitation mentioned by Kalkofen et al. (1994). These authors analytically derive a $t^{-1/2}$ law for pulse excitation as opposed to the $t^{-3/2}$ law for continuous excitation. This is not found in our calculations (see Fig. 15, but also Figs. 7, 9, 11, 12). We invariably found for the pulse excitation an exponential decay law, with the same damping rate as for the continuous wave excitation case. For this reason we have rederived the pulse case analytically (Sutmann 1994, in preparation) and found a $t^{-3/2}$ law which as discussed above is in good agreement with the exponential case and our numerical simulations.

The difference between our result and that of Kalkofen et al. apparently lies in the way the pulse excitation is applied (Massaglia 1994, private communication). While we apply the pulse by a temporal piston motion which stops after a given time span (see Eq. (2)), a motion which is intended to simulate a sudden disturbance arriving at the bottom of the atmosphere, Kalkofen et al., following Lamb (1908), set an initial condition at time $t = 0$, assuming for the perturbation a δ-function-like dependence in space.

5. Conclusions

The time-dependent numerical simulations of the response of solar atmosphere models to various linear excitations lead to the following conclusions.

1. Continuous excitation in isothermal atmospheres by waves with incident frequencies both above and below the cut-off frequency ν_A leads to strong resonances at ν_A. The resonances are stronger at greater atmospheric height. For progressively later times the resonance oscillations die out following an exponential law, only the incident wave survives. Although our results show an exponential behaviour, they are in qualitatively good agreement with the analytical $t^{-3/2}$ power-law results of Kalkofen et al. (1994) (see Fig. 15). We suspect, however, that the analytic solution suffers from crude assumptions and that the exponential decay is correct.
2. For a pulse excitation of the isothermal atmosphere we find a similar behaviour as for the continuous excitation. In particular we find the same exponential decay law. This is supported by an analytical derivation (Sutmann 1994, in preparation) which yields the $t^{-3/2}$ power law.
3. Excitation of an atmosphere with a constant negative temperature gradient leads to a qualitatively similar response. Both for continuous and pulse excitation an exponential decay of the resonance is obtained, however, the decay rate now is much slower than in the isothermal atmosphere. A common resonance frequency is found which corresponds to the average height of the atmosphere.
4. For atmospheres with a constant positive temperature gradient, both for continuous and pulse excitation, a very rapid exponential decay of the resonance is found, quite unlike to the cases of the isothermal and negative gradient atmospheres. In addition, for the positive gradient case the amplitude of the initial resonance disturbance is much reduced compared to that in the other cases. A common resonance frequency is found corresponding to the lowest, most massive layer.
5. The response of the Vernazza et al. model C is similar to the positive gradient case. A very rapid exponential decay is seen for the resonance, both for continuous wave and pulse excitation. After some time this resonance has a common frequency near ν = 5 mHz. The resonance behaviour of the model is very different from that of an isothermal atmosphere model.

6. From a spectrum introduced at the bottom of the atmosphere containing both propagating and evanescent components, only the propagating component survives the passage through the atmosphere. The chromosphere can thus be seen as a high pass frequency filter.
7. Stochastically generated wavetrains are able to generate stochastically appearing resonance oscillations at the cut-off frequency. Each change in frequency is associated with a new resonance oscillation episode together with its subsequent decay.

References

Courant R., Hilbert, D.: *Methods of Mathematical Physics II*, John Wiley, New York

Deubner F.-L. 1991, in: *Mechanisms of Chromospheric and Coronal Heating*, Ulmschneider P., Priest E.R., Rosner R., Eds., Springer, Berlin, p. 6

Fleck B., Schmitz F.: 1991, A&A **250**, 235

Fleck B., Schmitz F.: 1993, A&A **273**, 671

Kalkofen W., Rossi P., Bodo G., Massaglia S.: 1994, A&A **284**, 976

Lamb, H.: 1908, Proc. London Math. Soc. 7, 122

Lamb, H.: 1932, *Hydrodynamics*, Dover Publ., New York

Leighton R., Noyes R., Simon G.W.: 1962, ApJ **135**, 474

Leibacher J.W., Stein R.F.: 1981, in: *The Sun as a Star*, Jordan S., Ed., NASA SP-450, p. 263

Morse P.M., Feshbach H.: 1953, *Methods of Theoretical Physics*, Part I, Mc Graw Hill, New York

Rammacher W., Ulmschneider P.: 1992, A&A **253**, 586

Rutten R.J., Uitenbroek H.: 1991, Solar Phys. **134**, 15

Sutmann G. Ulmschneider P.: 1994, A&A, same issue

Ulmschneider P., Kalkofen W., Nowak T., Bohn H.U.: 1977, A&A **54**, 61

Ulmschneider P., Muchmore D., Kalkofen W.: 1987, A&A **177**, 292

Vernazza J.E., Avrett E.H., Loeser R.: 1981, ApJS **45**, 635

This article was processed by the author using Springer-Verlag TEX A&A macro package 1992.